Size-Dependent Ultrafast Ionization Dynamics of Nanoscale Samples in Intense Femtosecond X-Ray Free-Electron-Laser Pulses

Sebastian Schorb, Daniela Rupp, Michelle L. Swiggers, Ryan N. Coffee, Marc Messerschmidt, Garth Williams, John D. Bozek, Shin-Ichi Wada, Oleg Kornilov, Thomas Möller, and Christoph Bostedt

Phys. Rev. Lett. **108**, 233401 — Published 4 June 2012

DOI: 10.1103/PhysRevLett.108.233401

Size-dependent ultrafast ionization dynamics of nanoscale samples in intense femtosecond x-ray free-electron laser pulses

Sebastian Schorb,[1] Daniela Rupp,[2] Michelle L. Swiggers,[1] Ryan N. Coffee,[1] Marc Messerschmidt,[1] Garth Williams,[1] John D. Bozek,[1] Shin-Ichi Wada,[1,3] Oleg Kornilov,[4] Thomas Möller,[2] and Christoph Bostedt[1]

[1]*Linac Coherent Light Source, SLAC National Accelerator Laboratory, Stanford, California 94309, USA*

[2]*Institut für Optik und Atomare Physik, Technische Universität Berlin, Hardenbergstr. 36, 10623 Berlin, Germany*

[3]*Department of Physical Science, Hiroshima University, 1-3-1 Kagamiyama, Hiroshima 739-8526, Japan*

[4]*Max-Born-Institute, Max-Born-Str. 2, 12489 Berlin, Germany*

(Dated: April 5, 2012)

Abstract

All matter exposed to intense femtosecond x-ray pulses from the Linac Coherent Light Source (LCLS) free-electron laser is strongly ionized on time scales competing with the inner-shell vacancy lifetimes. We show that for nanoscale objects the environment, i.e., nanoparticle size, is an important parameter for the time-dependent ionization dynamics. The Auger lifetimes of large Ar clusters are found to be increased compared to small clusters and isolated atoms due to delocalization of the valence electrons in the x-ray induced nanoplasma. As a consequence, large nanometer sized samples absorb intense femtosecond x-ray pulses less efficiently than small ones.

PACS numbers: 36.40.Gk, 36.40.Mr, 32.80.Hd, 52.50.Jm

Intense x-ray flashes from free-electron laser sources such as the Linac Coherent Light Source (LCLS) [1] open the door for a wide range of novel applications ranging from ultrafast time-resolved x-ray spectroscopy to single-shot imaging of nanometer-sized objects. All matter irradiated by femtosecond x-ray pulses with fluences in excess of 10^5 Photons/Å^2 will become highly ionized and the detailed ionization dynamics are a subject of intense current research [2–6].

First experiments at LCLS have focussed on the investigation of ionization dynamics of atoms [2] and small molecules [3, 4] in intense x-ray pulses. However, for extended nanometer-scaled systems theory predicts that there is a strong influence of the environment, i.e., particle size, on the ionization dynamics in intense x-ray pulses [7]. The charges created by the x-ray pulse lead to delocalization of the valence electrons and subsequently to a reduction of the Auger rates.

Atoms in intense x-ray pulses are sequentially ionized from the inside out starting with the inner-shell electrons which exhibit the highest absorption cross section in the x-ray regime. Until the inner-shell vacancy is filled the sample becomes transiently more x-ray transparent, which is also referred to as core-level bleaching. The overall sample absorption depends sensitively on the x-ray pulse length and inner-shell vacancy lifetimes [2].

The absorption of intense x-ray pulses in nanometer-sized systems is driven by the same fundamental processes but additional effects become important. First the inner-shell electrons of the atoms are removed by the x-ray pulse. After a certain number of ionization events the particle is charged to a degree that its Coulomb energy becomes higher than the kinetic energy of the ejected electrons. Subsequently the Auger and photoelectrons are trapped in the particle's Coulomb potential [8, 9] and a dense nanoplasma is formed [10]. The nanoplasma will disintegrate into ionic fragments carrying kinetic energy with possible recombination of the nanoplasma core [11, 12].

In this letter we report on time-dependent ionization dynamics of nanoscale samples in intense x-ray pulses with power densities up to $10^{17}\,\mathrm{W/cm^2}$. We introduce a new method to measure time-dependent components of ultrafast x-ray absorption. Our data reveal a strong influence of the environment, i.e., particle size on the absorption. This is attributed to delocalization of the valence electrons stemming from barrier suppression in the multiply charged particle and therefore effectively reducing the Auger rates. As a consequence larger samples absorb the intense x-rays less efficiently.

The experiments were performed at the AMO-HFP endstation [13] of the LCLS [1]. X-ray pulses with a photon energy of 480 eV were focussed down to a spot size of 1.2 μm^2. To measure the time-dependent component of the absorption, the x-ray pulse length was dynamically tuned between 30 fs and 85 fs using the slotted spoiler foil in the LCLS accelerator [14]. This foil allows controlling the length of the lasing part of the electron bunch by spoiling the emittance of the remaining electrons. By that means the x-ray pulse length can be continuously and precisely tuned at the expense of overall pulse energy. The x-ray pulse energies were measured with gas detectors after the undulator [15] which were calibrated to the electron beam energy loss due to the FEL process [1]. As sample system Ar nanoclusters were chosen. Ar is a monoatomic gas and clusters can reliably be produced from it. Further, Ar has been also used in the model calculations by Saalmann et al. [7] At 480 eV photon energy the Ar L-shell electrons exhibit the highest absorption cross section. Atomic clusters are ideal for the present investigation because their size can be easily tuned. Further, they can be produced in sufficient density for measurements in the gas-phase for which any influence from a surrounding medium or sample support can be excluded. The clusters were produced with a pulsed valve by supersonic expansion of Ar gas through a 100 μm conical nozzle with an opening half angle of 15 °. Their size was tuned from $\langle N \rangle = 1$ to 1600 by changing the backing pressure between 1 and 13 bar according to the Hagena scaling laws [16, 17]. The cluster jet passes through two differentially pumped skimmer stages in order to produce a defined target. The Ar cluster target was crossed with the FEL beam above the aperture of a time-of-flight (tof) spectrometer.

In Fig. 1 tof spectra of Argon cluster with an average size of $\langle N \rangle = 1600$ are shown for two different x-ray pulse length (30 fs and 85 fs) and an x-ray pulse energy of 0.15 mJ. The peaks in the spectrum consist of the individual Ar ions from the cluster explosion. The inset in Fig. 1 shows an atomic Argon spectrum for the same pulse energy and an x-ray pulse length of 50 fs. In the atomic spectrum we observe charge states up to Ar^{13+}. The ground state ionization potential of Ar^{11+} is with ≈ 570 eV already higher than the photon energy, indicating that multiple ionization via resonant excitation and intermediate excited states occurs.

For the atomic and cluster spectra (c.f. Fig. 1), two main differences can be observed. First, the average measured charge states are lower in the cluster than in the atom due to the charge trapping and subsequent nanoplasma recombination in the cluster expansion

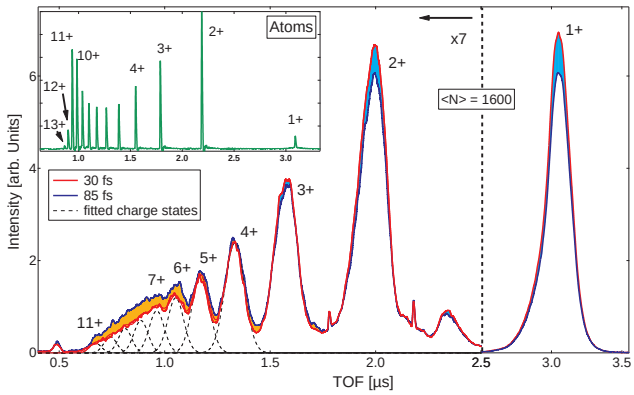

FIG. 1. Time-of-flight spectra from argon clusters with a size of $\langle N \rangle = 1600$ atoms for 30 fs and 85 fs x-ray pulse length and 0.15 mJ pulse energy. The difference between long and short pulses is indicated in orange (higher intensity for long pulses) and blue (higher intensity for short pulses). The dashed lines indicate the assignment of the different charge states. Inset: Atomic argon time-of-flight spectrum for the same pulse energy and 50 fs pulse length. Compared to the atomic spectrum the ion peaks from the cluster are shifted and broadened due to the kinetic energy release from the cluster explosion.

and cooling phase. Second, the measured ion peaks in the cluster spectra are shifted and broadened due to the kinetic energy release of the cluster fragments stemming from the cluster explosion. These secondary effects affecting the cluster spectra are slow compared to the femtosecond pulse length [18] and fundamentally the same overall cluster absorption leads to the same spectra.

Comparing the two cluster spectra in Fig. 1 recorded with different x-ray pulse length, small but important differences become apparent. For the 30 fs pulse the yield of low charge states is higher and the yield of high charge states is lower compared to the 85 fs pulse. In more detail, for the shorter pulse the Ar^{+} and Ar^{2+} peaks are increased by the blue shaded area and the charges states of Ar^{6+} and above are decreased as indicated by the yellow shaded area. Ar^{3+} to Ar^{5+} exhibits similar intensities. Generally spoken, these differences lead to a decreased average charge state for the short pulse spectrum. Qualitatively the observed behavior is similar to the x-ray pulse length dependencies observed in atomic targets [2] and the presently recorded atomic Ar spectra show similar trends.

Discussing the absorption dynamics of clusters in intense laser pulses poses the difficulty that the spectra from different cluster sizes are not directly comparable to each other due to

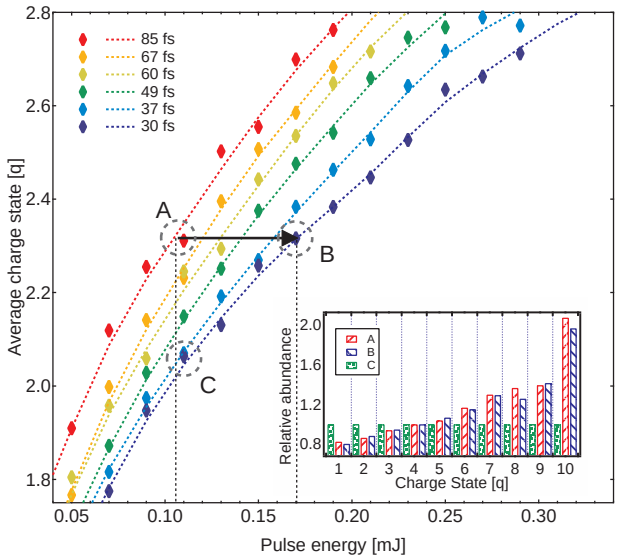

FIG. 2. Average charge state of the detected ionic cluster fragments vs. x-ray pulse energy for clusters with an average size of $\langle N \rangle = 1600$ atoms. The different colors indicate different pulse length. The diamond shaped markers are binned data points and the dashed lines interpolated curves. The black horizontal arrow marks the XITI from a 30 fs to a 85 fs pulse. Inset: Abundances of charge states at point A, B and C. For better visibility single charge states are normalized to the value of point C.

the secondary processes affecting the tof spectra. To overcome this hurdle we take advantage of the fact that the secondary processes are slow compared to the femtosecond x-ray pulse. Therefore the same number of absorbed photons will lead to the same final ion yield spectrum and thus, average charge state. By this means a measure for the time-dependent component of the absorption can be found for every cluster size as discussed in detail below. For the analysis of the cluster absorption as function of the x-ray pulse length the average charge states of clusters are determined from the ion yield spectra displayed in Fig. 1. Due to their kinetic energy, the cluster fragments with charges higher than 4+ can hardly be separated. To compute the average charge state from the tof spectra a SIMION simulation is used to fit higher charge states under the assumption of a quadratic increase in kinetic energy with ion charge state in good agreement with the data and earlier results [19].

In Fig. 2 the measured average charge state of a $\langle N \rangle = 1600$ cluster vs. the pulse energy for six different x-ray pulse lengths are plotted. Every data point is computed from an averaged tof spectrum containing a few hundred laser shots within a pulse energy bin of

$\Delta E = 0.02\,\mathrm{mJ}$. The dotted lines are interpolations of the data bins. In the data two trends are apparent: First, for constant pulse length the average charge state increases with increasing pulse energies (along each curve in Fig. 2). Second, for constant pulse energies the average charge state increases with longer pulses (going vertically up in the set of curves in Fig. 2). In the inset of Fig. 2 the ion yield distributions (i.e. spectra) for the three distinct points A, B, and C are compared. It shows that fundamentally the same average charge state for the example points A and B are generated by the same charge state distribution. To measure the same average charge state for a long (e.g. 85 fs, point A) and a short (e.g. 30 fs, point B) pulse, a higher pulse energy is needed for the short pulse. The horizontal arrow in Fig. 2 illustrates this difference in pulse energy. Specifically, for the $\langle \mathrm{N} \rangle = 1600$ cluster in Fig. 2, 60% more pulse energy, i.e., photons are needed to produce the same average charge state with a 30 fs pulse compared to a 85 fs pulse. In other words, an argon cluster of $\langle \mathrm{N} \rangle = 1600$ atoms is 60% more transparent for an intense 30 fs x-ray pulse compared to an 85 fs one. For the following discussion we define this as x-ray induced transparency increase (XITI) of 60% in a 30 fs pulse compared to a 85 fs pulse for a fixed initial pulse energy. It is pointed out that XITI is a measure for the time-dependent components in the absorption, i.e., the lifetime of the inner-shell vacancies. For Ar excited with intense 480 eV x-ray pulses the inner-shell vacancy lifetime and thus the XITI, is dominantly determined by the Auger rates.

To investigate the influence of the environment on the ultrafast x-ray absorption, similar data sets to the one exemplified in Fig. 2 have been acquired for an atomic target and four cluster sizes ranging from $\langle \mathrm{N} \rangle = 55$ to $\langle \mathrm{N} \rangle = 1600$. The XITI for the atom as well as the clusters for the same pulse length combination of 85 fs and 30 fs is summarized in Fig. 3. First and foremost, the XITI in Fig. 3 is much higher for all cluster sizes compared to the atom reference which can be directly attributed to changing Auger lifetimes in the clusters. The Auger lifetimes have been theoretically predicted by Saalmann et al. to change for clusters in intense x-ray pulses compared to atomic samples [7]. The atoms in the cluster are ionized by the x-ray pulse through inner-shell photoionization and Auger decay. As the positive cluster Coulomb potential increases the photo- and Auger electrons cannot leave the cluster any more. This massive creation of charges leads to suppression of the Coulomb barrier between the atoms in the cluster. At least the high laying valence electrons are then turned into quasi-free electrons and they are effectively delocalized. Consequently,

the overlap between these electrons and the localized inner-shell vacancies decreases and therefore the Auger rates are reduced [7].

Further, the XITI varies systematically within the different samples indicating a dependence of the Auger rates on the cluster size. The relative change of the Auger lifetime with the cluster sizes is encoded in the shape of the curve in Fig. 3 which can be explained as follows. If all Auger life times of the atoms in the cluster were very much smaller than the two used pulse lengths, the absorption process would not depend on them as all vacancies decay between two ionization events. Thus, the average charge states for both pulse lengths would be the same and the XITI would equal 0. Similarly, if all Auger life times were much larger than the pulse length, no decay would happen between two ionization events. Also in this case, the absorbtion process would not depend on the pulse length and the XITI would be again equal to 0. If the Auger lifetimes are such that they are close to the used pulse lengths, they play a role in the sequential absorption processes. In this case a shorter pulse will see a more transparent sample because on average the probability that the vacancies are filled is lower compared to a longer pulse. Therefore the XITI will be greater than 0 and it will depend sensitively on the Auger lifetimes.

To support the arguments above and further investigate the impact on Auger lifetimes

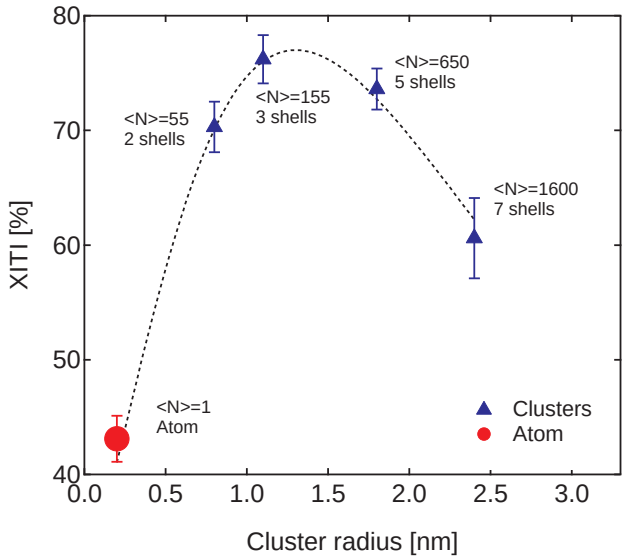

FIG. 3. XITI from 85 fs to 30 fs x-ray pulse length for atoms and different cluster sizes ranging from $\langle N \rangle = 55$ atoms (2 geometric shells) to $\langle N \rangle = 1600$ (7 geometric shells). The dashed line is a guide to the eye.

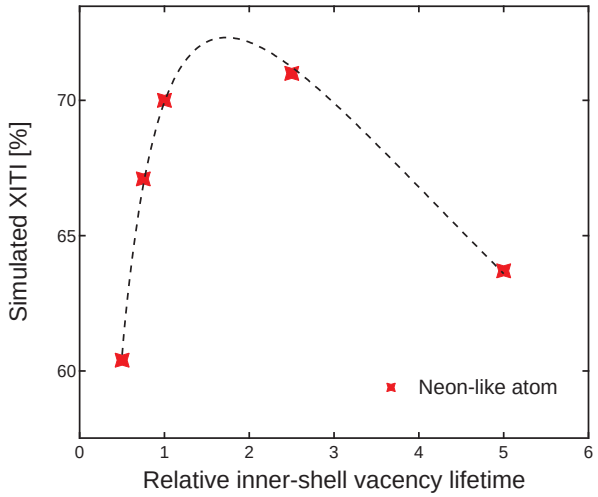

FIG. 4. Simulated XITI of an atomic Ne-like system. All lifetimes of the inner-shell vacancies are artificially tuned by the linear factors shown on the x-axis. The dashed line is a guide to the eye. The simulated XITI exhibits qualitatively the same shape as the cluster-size dependent XITI (c.f. Fig. 3 and goes through a maximum for intermediate lifetimes, indicating that different cluster sizes result in different inner vacancy lifetimes.

on the curve shape, the XITI of a simplified and well understood system as a function of inner-vacancy lifetimes is simulated with a rate equation model. Similar models have been used to describe the absorption of Ne atoms in intense x-ray pulses and they have matched the experimental data very well [2]. For Argon, however, multiple ionization via unknown intermediate excited states becomes important adding uncertainty to the simulations. Specifically, the unexpected high charge states above Ar^{11+} observed in the atomic spectra shown in Fig. 1 indicate that these processes play an important role under the current experimental conditions. Therefore Ne is chosen for this proof-of-principle simulation because all relevant rates and states are known. The absorption of Ne-like atoms for two different pulse length is calculated with a rate equation model. The Ne absorption cross sections are computed using the Los Alamos Atomic Physics Code [20] and the Auger and fluorescence rates are taken from the literature [21]. The FEL pulse is approximated with a Gaussian envelope function. With the rate equation model ion yields are calculated for different pulse length and pulse energies. From the results the XITI is determined as described above for the experimental data. To investigate the impact of the inner-shell vacancy lifetimes they are artificially varied in the calculations. The results of the simulations are shown in

Fig. 4. Overall, the shape of the simulated curve is very similar to the one deduced from the experimental data displayed in Fig. 3. Concurrent with the arguments outlined above, the XITI goes through a maximum for intermediate lifetimes and decreases for shorter as well as for longer lifetimes. The data in combination with the simulation show that in intense x-ray laser pulses the Auger lifetimes of nanoscale samples increase with size. This increase in Auger lifetime results in decreased absorption.

While a quantitative statement about the increase of Auger lifetimes in the Ar clusters is difficult without detailed calculations, a crude estimate can be given. If the XITI is assumed to be linear between a lifetime of zero and the maximum, the measured increase by a factor two from the atom to $\langle \mathrm{N} \rangle = 155$ in Fig. 3 can be translated to a factor two increase in average lifetimes as a lower limit. This is in good agreement with the factor five predicted by the calculations of Saalmann et al. for slightly different pulse conditions [7].

The present investigation shows that the ionization dynamics in intense x-ray pulses are strongly influenced by the environment because the inner-shell vacancy recombination rates change compared to isolated atoms. These results have important implications for a wide range of experiments using intense x-ray pulses. In single-shot imaging the photo absorption damage limits the usable fluence. Very high fluences can be used to record meaningful scattering images if the pulse length is short compared to the Auger lifetimes of the sample [22]. Through the increased Auger lifetimes in nanometer-sized samples the radiation damage may be lower than predicted. Further, in dense x-ray excited plasmas inner-shell ionization and subsequent Auger decays play an important role [6, 23]. Understanding the environmental influence on the ionization dynamics could help to develop more sophisticated models for such matter in extreme conditions. Double core-hole spectroscopy has been proposed to greatly increase the sensitivity in chemical analysis [24, 25]. The lifetimes of the inner-shell holes are the decisive parameters for these investigations as they determine the core hole abundance for a certain pulse intensity. For larger systems the influence of the environment and the additional changes in the valence electrons through ionization will have to be taken into account.

In conclusion the ionization dynamics of nanoscale systems in intense x-ray pulses are strongly influenced by the environment. Measuring the x-ray induced transparency increase XITI with ultrafast pulse length dependent absorption shows that the Auger lifetimes increase for nanoparticles compared to atomic targets as well as with increasing particle size.

The increase in Auger lifetimes stemming from delocalization of the valence electrons in the massively ionized cluster leads to lower absorbtion due to core-level bleaching. We expect the effect to be important for a wide range of experiments at free-electron laser sources making use of the high power densities, ranging from damage models for single-shot imaging to dynamics of dense plasmas.

This research was carried out at the Linac Coherent Light Source, a national user facility operated by Stanford University on behalf of the U.S. Department of Energy, Office of Basic Energy Sciences. D.R. and T.M. acknowledge financial support from BMBF grant 05K10KT2.

[1] P. Emma et al., Nat. Photonics **4**, 641 (2010).

[2] L. Young et al., Nature **466**, 56 (2010).

[3] J. P. Cryan et al., Phys. Rev. Lett. **105**, 083004 (2010).

[4] M. Hoener et al., Phys. Rev. Lett. **104**, 253002 (2010).

[5] G. Doumy et al., Phys. Rev. Lett. **106**, 083002 (2011).

[6] S. M. Vinko et al., Nature **482**, 59 (2012).

[7] U. Saalmann and J. M. Rost, Phys. Rev. Lett. **89**, 143401 (2002).

[8] C. Bostedt et al., Phys. Rev. Lett. **100**, 133401 (2008).

[9] H. Iwayama et al., J. Phys. B **42** (2009).

[10] C. Bostedt et al., New J. Phys. **12**, 083004 (2010).

[11] M. Hoener et al., J. Phys. B **41**, 181001 (2008).

[12] H. Thomas et al., Phys. Rev. Lett. **108**, 133401 (2012).

[13] J. D. Bozek, Eur. Phys. J. **169**, 129 (2009).

[14] P. Emma et al., Phys. Rev. Lett. **92**, 074801 (2004).

[15] S. P. Hau-Riege et al., Phys. Rev. Lett. **105**, 043003 (2010).

[16] O. F. Hagena and W. Obert, J. Chem. Phys. **56**, 1793 (1972).

[17] U. Buck and R. Krohne, J. Chem. Phys. **105**, 5408 (1996).

[18] C. Bostedt et al., Phys. Rev. Lett. **108**, 093401 (2012).

[19] H. Thomas et al., J. Phys. B **42**, 134018 (2009).

[20] Los Alamos National Laboratory Atomic Physics Codes, http://aphysics2.lanl.gov/cgi-bin/ION/runlanl08a.pl.

[21] C. P. Bhalla, N. O. Folland, and M. A. Hein, Physical Review A **8**, 649 (1973).

[22] S.-K. Son, L. Young, and R. Santra, Phys. Rev. A **83**, 033402 (2011).

[23] B. Nagler et al., Nat. Physics **5**, 693 (2009).

[24] L. Cederbaum, F. Tarantelli, A. Sgamellotti, and J. Schirmer, J. Chem. Phys. **85**, 6513 (1986).

[25] N. Berrah et al., P. Natl. Acad. Sci. USA **108**, 16912 (2011).